Meddies and Their Sea Surface Expressions: Observations and Theory

FEDERICO IENNA,[a,b] IGOR BASHMACHNIKOV,[c,d,e] AND JOAQUIM DIAS[a,b]

[a] *Marine and Environmental Sciences Center, Faculdade de Ciências, Universidade de Lisboa, Campo Grande, Lisbon, Portugal*
[b] *Departamento de Engenharia Geográfica, Geofísica e Energia, Faculdade de Ciências, Universidade de Lisboa, Campo Grande, Lisbon, Portugal*
[c] *Department of Oceanography, St. Petersburg State University, St. Petersburg, Russia*
[d] *Nansen International Environmental and Remote Sensing Centre, St. Petersburg, Russia*
[e] *Marine Hydrophysical Institute of Russian Academy of Sciences, Sebastopol, Russia*

(Manuscript received 7 April 2022, in final form 7 June 2022)

ABSTRACT: The sea surface expressions of Mediterranean Water eddies, known as "meddies," are observed in satellite data, and their main characteristics are measured. Satellite altimeter observations of surface expressions are detected over the meddies observed in situ using the MEDTRANS meddy dataset (1950–2013). In this study 209 observed meddy cores in the North Atlantic Ocean, selected over the period of the 22 years of sea surface height measurements with satellite altimetry (1993–2013), were analyzed. Results show relatively good agreement between the theoretical estimates of the meddy surface signals as reported by Bashmachnikov and Carton and the measured surface expressions. It was found that, on average, the theoretical results underestimate the measured sea surface elevations of the meddy surface expressions by a factor of 2. Although the variability of the measured expressions is reasonably well described by the combination of meddy core and the ocean background parameters of the theoretical expression, we cannot define a single individual parameter of the meddy core, which chiefly shapes the magnitude of the meddy surface signal. Interestingly, the overall distribution of characteristics of meddy surface expressions in the Atlantic shows that the sea level anomalies formed by meddies intensify westward, growing both in magnitude and radius. This opposes the expected theoretical decrease of meddy surface signals due to a known progressive decay of the meddy cores with distance from their generation region at the Iberian continental slope. This observed tendency is attributed to meddy interaction with the upper-ocean currents and other eddies (in particular in the region of the North Atlantic Current and Azores Current) that are not considered by the theory.

KEYWORDS: Eddies; Mesoscale processes; Ocean dynamics; Altimetry; In situ oceanic observations; Remote sensing

1. Introduction

Deep coherent vortices (DCVs) are prevalent, observable physical phenomena that occur throughout the ocean. Mesoscale DCVs are typically identified as those with horizontal scales from one to several local baroclinic Rossby deformation radii (resulting in DCV radii within the order of tens of kilometers in the vast majority of cases). Being the result of baroclinic instability of the major ocean currents, mesoscale DCVs typically contain the highest amount of eddy kinetic energy in comparison with other mesoscale ocean dynamics (Cushman-Roisin and Beckers 2010). In the subtropical and tropical latitudes, mesoscale DCVs are large enough to be subject to relatively intensive self-propagation and are often observed to propagate against the mean flow (Vandermeirsch et al. 2001). Weak decay permits mesoscale DCVs to survive in the ocean from several months to over a year and transport water throughout the ocean and far from their point of origin (Chelton et al. 2011; Schouten et al. 2000). Whether through a final rapid destruction or through a slow exchange across their boundaries, DCVs release water from their cores into the surroundings, directly affecting the environment and serving as efficient mechanisms for transporting salinity, temperature, and other water properties over large distances (Richardson et al. 2000).

Mediterranean Water eddies—a specific type of DCV also known as "meddies"—are subsurface mesoscale anticyclones that offer excellent insight into the behavior of such dynamic entities because of their observability as pronounced thermohaline anomalies at middepths. Meddies in the northeastern Atlantic Ocean separate from the Mediterranean Undercurrent (MUC), which is formed by the outflow of the dense Mediterranean Water from the Gibraltar Strait, rapidly sinks to a neutral buoyancy depth of approximately 1000 m, and then propagates northward around the Iberian Peninsula. Observations suggest that meddy formation occurs most often at several locations off the Iberian coast: Cape St. Vincent, the Portimão Canyon, the Estremadura Promontory, and the Porto and Aveiro Canyons. Meddy formation as a result of the MUC interaction with capes and canyons can go through several different mechanisms (see, e.g., D'Asaro 1988; Pichevin and Nof 1996; Aiki and Yamagata 2004). In the cited studies the meddy generation from the MUC was suggested to go through barotropic or baroclinic instability of the MUC, while the separation from the MUC is triggered or enhanced by the flow interaction with the sharp bathymetry. After separating from the MUC, the newly generated DCVs become subject

Denotes content that is immediately available upon publication as open access.

Corresponding author: Federico Ienna, fienna@fc.ul.pt

DOI: 10.1175/JPO-D-22-0081.1

to their own internal dynamics and travel away from the coast, self-propagating westward, often against the mean current (Richardson et al. 2000; Bashmachnikov et al. 2015a). In the Atlantic, meddies can persist for periods from months to years, typically existing for less than 1–2 years (Richardson et al. 2000; Bashmachnikov et al. 2015a).

Typically, meddies contain a positive temperature anomaly of up to 4°C and a salinity anomaly of up to 1 unit, making their presence readily recognizable in vertical profiles (Richardson et al. 2000). Richardson et al. (1989, 1991) proposed a set of criteria for identification of a meddy: salinity anomaly over 0.2 (0.4 in the earlier study) in the depth range of 500–1500 m, which is generally considered to be the standard. Because of their relatively large radii (20–60 km) and pronounced positive temperature and salinity anomalies in their cores, a large number of meddies have been well documented in a rich observational history.

The first published observation of a DCV of Mediterranean Water was made in the Gulf of Cadiz, near the MUC, on a hydrographic survey by Swallow (1969), who observed a distinct anticyclonically rotating blob of deep Mediterranean Water. A similar observation was published by Piip (1969) in the same year, near the Madeira–Canaries region. Since then, several cruises have confirmed a regular emergence of such structures in the Canary Basin (see, e.g., Armi and Zenk 1984). In 1978, McDowell and Rossby (1978) observed a Mediterranean Water eddy as far as in the vicinity of the Bahamas and coined the term *meddy* to distinguish this specific type of eddies, generated from the Mediterranean Outflow in the Atlantic. Armi and Stommel (1983) detected another meddy near the Mid-Atlantic Ridge (MAR) southwest of the Canary Islands. One of the meddies, reported by Armi and Zenk (1984), was tracked over two years using neutral buoyancy floats, and its gradual decay was measured with repeated oceanographic sections (Armi et al. 1989; Hebert et al. 1990). Further on, several meddies were tracked from their generation sites in the MUC during the in situ RAFOS-tracking program known as A Mediterranean Undercurrent Seeding Experiment (AMUSE) (Bower et al. 1997). Another set of meddies was tracked for 6–11 months south on the Azores, at distances over 1000 km from the Iberian coast, during Structure des Echanges Mer-Atmosphère, Propriétés des Hétérogénéités Océaniques: Recherche Expérimentale (SEMAPHORE) (Richardson and Tychensky 1998; Tychensky and Carton 1998), among other programs. These and other studies (Paillet et al. 1999, 2002; Pingree 1995; Shapiro et al. 1995; Richardson et al. 2000; Carton et al. 2002; Demidov et al. 2012; Bashmachnikov et al. 2015a) have furthered knowledge on meddy formation sites, pathways, and the evolution of their cores over time.

Meddies propagate in the ocean because of the generation of secondary circulations as a result of a variation of the Coriolis parameter across the meddy core (Cushman-Roisin et al. 1990; Morel and McWilliams 1997), producing a predominantly westward eddy self-propagation mechanism. Other secondary effects in the dynamics of the propagating eddies, together with the background currents and topography often add a meridional (typically southward) component to the meddy motion.

Meddies influence the physical and chemical properties, as well as the stratification of the water column from the upper ocean to, at least, 2000 m (Mauritzen et al. 2001). As such, meddies are known to be an important contributor to the westward and southwestward transport of Mediterranean Water from the Iberian margin, contributing between 50% and 100% to the formation of the Mediterranean salt tongue in the Atlantic (Arhan et al. 1994; Bower et al. 1997; Mazé et al. 1997; Sparrow et al. 2002).

Despite having the upper limit of their thermohaline cores at around 500 m, meddies are known to consistently transmit their dynamic signal to the ocean surface. In what was perhaps the first published mention of meddies' manifestation at the sea surface, Käse and Zenk (1987) demonstrated a tendency of a surface drifter to make a semicircle in a clockwise direction over an observed meddy. Since then, ample evidence of meddies forming a measurable dynamic signature at the sea surface has been collected (Stammer et al. 1991; Pingree and Le Cann 1993a; Oliveira et al. 2000; Paillet et al. 2002; Bashmachnikov et al. 2009; Jo et al. 2015; Ciani et al. 2015, among others).

A meddy's surface expression results from the lifting of isopycnals throughout the water column above the meddy core. A propagating meddy that travels at a neutral buoyancy level throughout the ocean causes a compression of the water column above the frontal part of its core relative to the direction of its propagation (Fig. 1). By conservation of potential vorticity, this compression induces an anticyclonic rotation in the upper ocean, causing isopycnal lifting that may propagate all the way to the sea surface. This mechanism may force the lifting the sea surface as much as 15–20 cm in the most extreme cases. By geostrophy, this implies a sea surface anticyclonic rotation with azimuthal velocity often exceeding 10 cm s^{-1}. This effect has been observed in satellite altimetry sea level measurements (Stammer et al. 1991; Oliveira et al. 2000; Bashmachnikov et al. 2009, 2013, 2015a; Ienna et al. 2014), direct sea surface velocity measurements (Armi et al. 1989; Bower et al. 1997), and in high-resolution model results (Serra et al. 2002; Ciani et al. 2015). Detailed in situ observations in the subtropics have confirmed that the entire water column above a meddy rotates anticyclonically. The rotation velocity gradually decreases upward and, at the sea surface, typically forms up to 30% of the maximum rotation velocity in the meddy core still reaching 10–25 cm s^{-1} (Armi et al. 1989; Pingree and Le Cann 1993a,b; Pingree 1995; Paillet et al. 2002; Bashmachnikov and Carton 2012; Bashmachnikov et al. 2013).

The close coupling of meddy cores and their surface expressions has been demonstrated in several recent studies (Bashmachnikov et al. 2009, 2013, 2015a; Ienna et al. 2014). Yan et al. (2006) used satellite altimetry to observe the trends in the Mediterranean Outflow through its surface effects, which included the surface effects of meddies. Bashmachnikov and Carton (2012), and later Bashmachnikov et al. (2014) and Ciani et al. (2017), derived theoretical expressions for the intensity of meddy surface signals as a function of meddy core properties and environmental conditions, for different patterns of potential vorticity anomalies in and around a meddy core. Testing the theoretical results against surface expressions of several observed (or modeled) meddies suggests a validity of

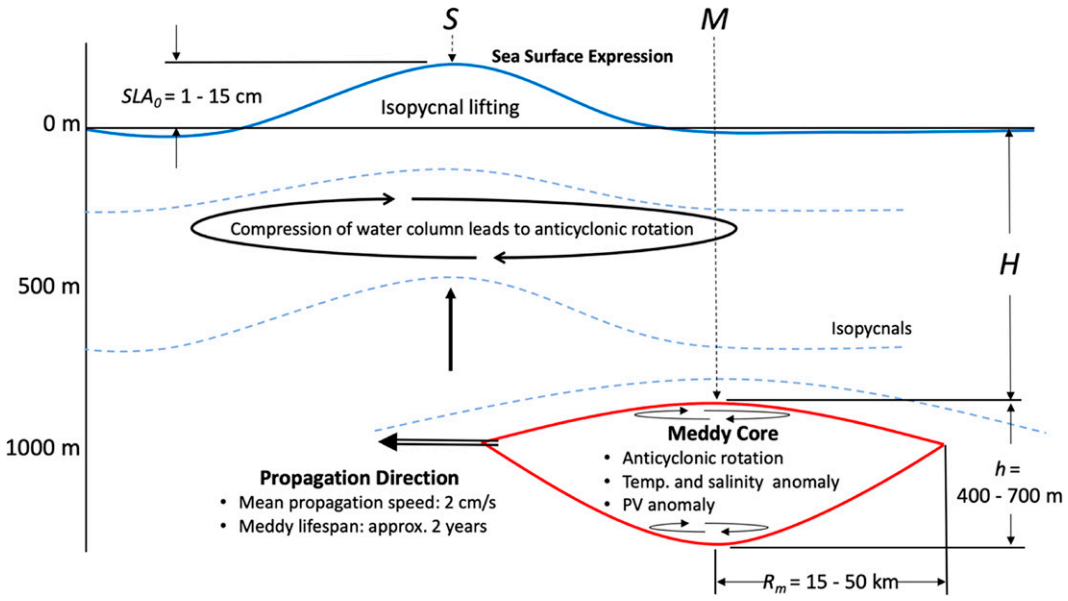

FIG. 1. Schematic representation of a formation process of the sea surface expression above a meddy core. The centers of the surface signal (*S*) and of the meddy core (*M*) are indicated.

these theoretical approaches. These studies also found a potential southern limit for detection of meddies with different radii and depths of the cores in satellite altimetry: approximately at 25°N for larger meddies and at around 35°N for smaller meddies. Meddies (Aiki and Yamagata 2004; Barbosa Aguiar et al. 2013) and their surface expressions (Ciani et al. 2015) have recently been rigorously treated in high-resolution model studies.

The results of the theoretical investigations above have only been tested against a few actual observations. In this study, we present the first consistent analysis of the spatial variability of surface expressions of 209 meddies, observed throughout the northeastern Atlantic since 1993, and compare these with the theoretical estimates from Bashmachnikov and Carton (2012). The meddy cores used herein, detected in situ in Argo profilers and CTD casts, are derived from the Mechanisms of Transport and Dispersion of the Mediterranean Water in the Subtropical Northeast Atlantic (MEDTRANS) dataset as described in Bashmachnikov et al. (2015a), and their surface expressions are detected in Archiving, Validation and Interpretation of Satellite Oceanographic data (AVISO) satellite altimetry. This results in a further refinement of our understanding of the potential ties between surface expressions and physical and dynamic parameters of deep meddy cores, and how they are affected by the background ocean. The data used and the method for matching surface-to-core are discussed in section 2. A statistical analysis of the meddy surface expressions is presented in section 3, followed by an analysis of the geographical patterns observed in the distribution of properties of the surface expressions themselves. The results are the discussed in section 4.

2. Method

In situ salinity and temperature profiles are used for detection of the meddy cores. Remote sensing data from altimeter-derived sea surface height (SSH) are used to detect sea level anomalies representing surface signals of these meddies. The combination of deep in situ and satellite surface observations, taken over the same time period, allows us to link meddy core parameters to their surface signature.

a. *In situ data*

The in situ positions and properties of the detected meddies (1970–2014) were previously derived in the MEDTRANS project (Bashmachnikov et al. 2015a). Temperature and salinity from vertical profiles of Nansen bottles, conductivity–temperature–density probes (CTD, XCTD), and Argo profiling drifters from the World Ocean Database (WOD) were quality controlled in the framework of this project (Bashmachnikov et al. 2015b). Middepth temperature and salinity anomalies for identification of meddies were derived relative to MEDTRANS reference climatology (Bashmachnikov et al. 2015b,c), which includes the gridded 3D thermohaline distributions at 30-km spatial and 25-m depth intervals, available within a repository at the University of Lisbon (http://www.mare-centre.pt/en/research/data-library/medtrans-data).

The meddy cores were identified within in situ data using a slightly relaxed Richardson's criterion (Richardson et al. 1991), according to which a meddy core should form a salinity anomaly of at least +0.2 when averaged within the depth limits of 700 and 1300 m. Only meddies having been sampled with at least three profiles within the core were used for the analysis. Additionally, every radial distribution of the profiles within the selected meddies was double-checked by human eye, allowing for the filtering out of erroneous profiles, as well as eliminating the structures that do not have the distinguishable, typical lens shape of a meddy, despite having technically fit the criterion [see Bashmachnikov et al. (2015a, their section 2.2), for a

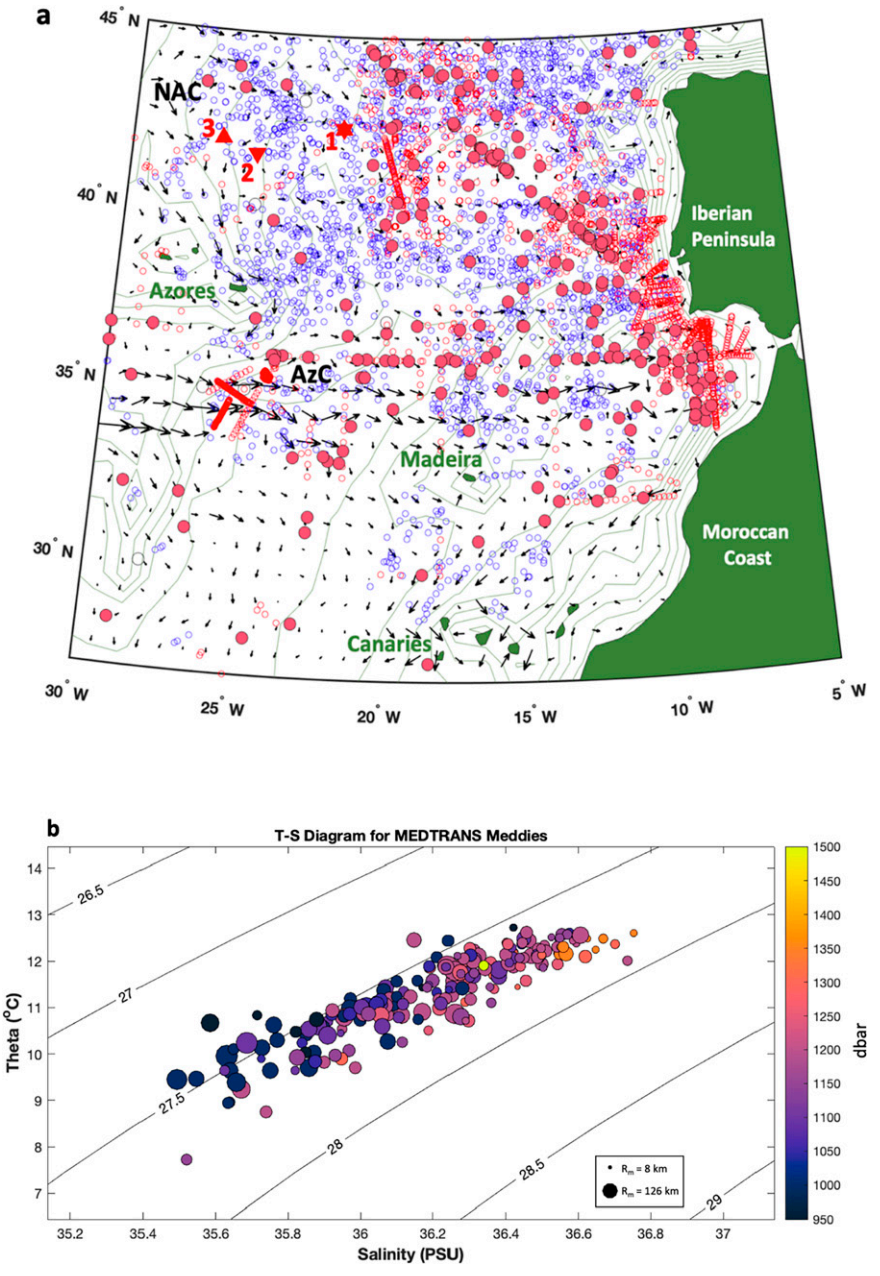

FIG. 2. (a) Distribution of all in situ meddy core observations during 1993–2014 that were used in this study. Red open circles are CTD and XCTD casts (68 meddies and 2261 profiles); blue open circles are Argo casts (294 meddies and 2551 profiles). The larger purple filled circles are a subset of MEDTRANS meddies with further statistics of core properties and correspond to the same subset plotted in (b). The mean sea surface currents are shown in black, and the locations of the North Atlantic Current (NAC) and Azores Current (AzC) are marked. The positions of three meddies 1, 2, and 3 with exceptionally high SLA (see Fig. 7) are highlighted by red symbols. (b) Temperature–salinity diagram of meddy cores used in this study; black lines are σ_θ (kg m^{-3}). The circle dimensions show radii (km) of meddy cores, and meddy core depths (dbar) are marked in color (in the case of double cores, the lower cores are selected).

detailed description of how the coordinates of meddy centers M and meddy radius R_m are derived from in situ data]. In this study, we use 209 meddy cores from the aforementioned MEDTRANS dataset detected in situ since 1993 (the beginning of the satellite altimetry era). The number of profiles in these meddy cores ranges from 3 to 40 profiles, composed in total of 2261 ship CTD casts and 2559 Argo profiler casts (Fig. 2).

b. Remote sensing data

To observe the sea surface expressions of the detected meddies, we used satellite-derived level-4 blended SSH, obtained from the repository available at the AVISO database (available since 1993). These are weekly global maps gridded at 1/4° spatial resolution. Because AVISO altimetry data are merged from a number of along-track observations from several satellites (CNES 2016), the accuracy of the results depends particularly on the distance from the nearest satellite track to the point of interest, as well as on the time difference between the in situ observations and the dates of the nearest tracks, both of which vary over the study region and time range. This may be a source of a certain nonphysical noise in the amplitudes and radii of the observed sea surface eddy structures (Bashmachnikov et al. 2020).

In situ observations suggest the current velocities in the meddies from 10 to 30 cm s^{-1} (Pingree and LeCann 1993a,b; Pingree 1995; Paillet et al. 2002; Bashmachnikov et al. 2013, 2014). Taking the typical radii of the sea surface expressions of 30–50 km, the geostrophic sea level anomalies should range from 5 to 15 cm, within the along-track altimetry observations (Oliveira et al. 2000). This is above formal accuracy of AVISO altimetry data of 4 cm, and such eddies are well discernable in AVISO altimetry (Chelton et al. 2011). A number of previous studies have successfully used satellite altimetry to track meddy surface signals along with the meddy cores, indicating that altimetry is relevant for observation of this phenomenon (Oliveira et al. 2000; Yan et al. 2006; Bashmachnikov et al. 2009, 2013, 2014; Bashmachnikov and Carton 2012; Ienna et al. 2014; Jo et al. 2015, among others).

The region of interest for this study, confined between 5° and 35°W and between 25° and 45°N, is known for its moderate sea surface height variability (Sterlini et al. 2016), which is favorable for the detection of meddy surface signals, which often form the strongest of all anticyclonic signals in the vicinity of a meddy (see, e.g., Bashmachnikov et al. 2009).

c. Algorithm for detection of meddy sea surface signals

The algorithm for detection of meddy surface signals is intended to function as an objective method for associating known meddy occurrences (see above), to the nearest negative relative vorticity anomaly (positive sea level anomaly) occurring over a detected meddy core, as theory suggests is the case (Bashmachnikov and Carton 2012; Bashmachnikov et al. 2014; Ciani et al. 2017).

The algorithm starts by searching for the nearest track of a satellite pass to the spatial and temporal coordinates of a given in situ meddy core center M. The time interval between a satellite pass and an in situ meddy occurrence is at most 10 days. The algorithm then searches for all nearby Gaussian-like sea level anomalies in the neighboring along-track sea level profiles within one radial distance of the meddy core R_m, and finds their center points, defined as the location of the highest individual sea level peak.

Once the center of the potential anomaly peak is detected, the next step is to evaluate the extent of the Gaussian-like anomaly. The SSH field, derived from gridded AVISO altimetry dataset, is converted to relative vorticity ω_s under the traditional geostrophic approximation (Arbic et al. 2012; Vallis 2006):

$$\omega_s = \frac{\partial v}{\partial x} - \frac{\partial u}{\partial y} = \frac{g}{f}\left(\frac{\partial^2 \eta}{\partial x^2} + \frac{\partial^2 \eta}{\partial y^2}\right), \quad (1)$$

where u (zonal) and v (meridional) are the sea surface velocity components, respectively; η is the sea level height; g is the acceleration of gravity; and f is the Coriolis parameter.

For each selected region of negative relative vorticity, we define the *boundary of the SSH anomaly* as the distance from the peak sea level height (the first-choice eddy center S) to the surrounding contour of zero relative vorticity by looking for the closest zero point where $\omega_s = 0$ along eight equally distributed radial transects starting at the first-choice center. If no zero value is reached within a predefined maximum radial distance, the eddy boundary is fixed at the nearest inflection point in the relative vorticity profile (i.e., where $\partial^2\omega_s/\partial s^2 = 0$). When both criteria are satisfied along the segment, whichever one closest to the center S is treated as a boundary of the surface signal (see example in Fig. 3). Then the mean of the radial distances to the selected boundary points of the anomalous relative vorticity patch is called the "dynamic radius" of the surface signal R_s. This method has been described in detail in Bashmachnikov et al. (2017).

Once the surface signal of a particular meddy n is outlined, the following characteristics of the meddy surface are derived:

- the longitude and latitude of the center point of the meddy surface expression, denoted by S_n,
- the radius of the sea surface expression R_s,
- the magnitude of the sea level expression SLA_0,
- the separation between the center points of the meddy core M_n and the meddy surface signal S_n, denoted by δ, and
- the azimuthal direction of the segment drawn between the meddy core center M_n and the surface expression center S_n, denoted by α.

Once automatically processed, a subset of the surface expression measurements was further verified by human eye to verify the work performed by the algorithm and to ensure that there were no obvious lapses in the output.

3. Results

a. Properties of sea surface expressions of meddy cores

The analysis of the properties of the meddy sea surface signals shows an increase of the peak sea level anomaly above the meddy center SLA_0 with its dynamic radius R_s, whose dependence can be fitted by a quadratic function (Fig. 4a), in meters,

$$SLA_0 = 5.7 \times 10^{-9} R_s^2 - 3.4 \times 10^{-4} R_s + 7.8 \quad (2)$$

Here we only consider meddy sea surface expressions with $SLA_0 \geq SLA_{min}$, where SLA_{min} is the formal maximum accuracy of AVISO satellite altimetry, which ranges between

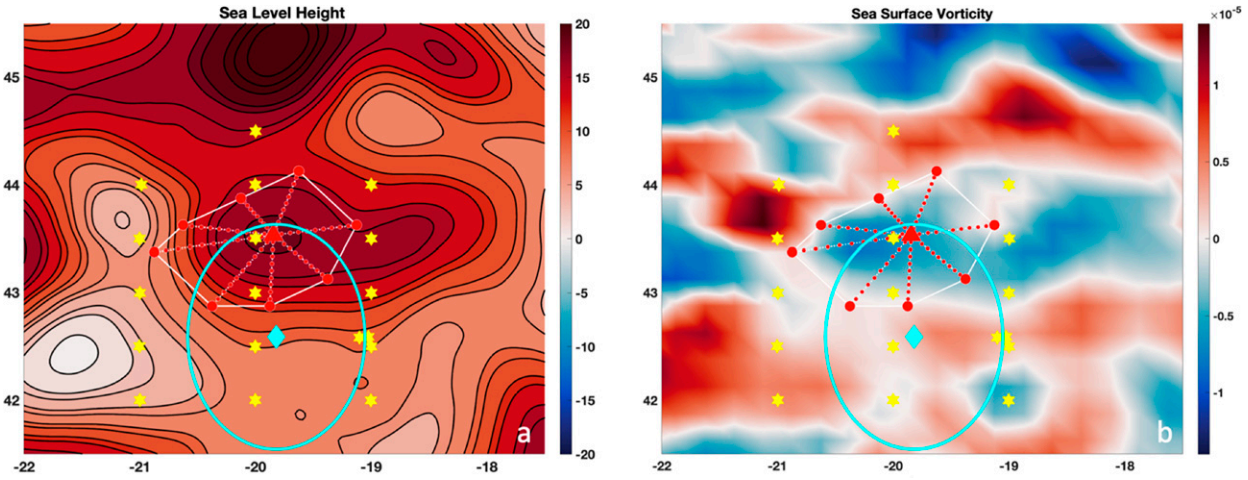

FIG. 3. An example of an identification of a meddy surface expression (a) in the SSH (cm) and (b) in the sea surface relative vorticity (s^{-1}). The meddy center M is marked with cyan diamond, and the cyan ellipse shows the meddy boundary (the dynamic radius). The location of all in situ measurements used to identify this meddy are shown as yellow stars. The location of the center of the sea surface anomaly S, identified as the meddy surface signal, is marked with the red triangle. The boundary of the sea surface signal is marked with the red point at the end of each of the dashed red radial segments. The final dynamic radius of the meddy surface signal R_s is the mean of the radial distances over all of the segments.

2 and 4 cm in the northeast Atlantic. The dependence between peak SLA_0 and R_s suggests a linear growth of the peak surface azimuthal velocity with R_s, consistent with a Rayleigh radial current profile. For meddy cores, the ratio of the azimuthal velocities to meddy radii (Rossby number in zonal bands) shows a rapid drop by about 50% within 300 km from the Iberian coast most likely due to frequent meddy mergers in the Iberian Basin (Bashmachnikov et al. 2015a). Farther away, meddy radii show a gradual decrease, nearly reaching the original values of, on average, 10–20 km over 2000 km from the coast (Bashmachnikov et al. 2015a). The overwhelming majority of the meddy sea surface signals discussed here are observed at distances of over 300 km from the Iberian coast and show an increase in R_s and of their surface azimuthal velocity [estimated from Eq. (2) using a geostrophic approximation] toward the Mid-Atlantic Ridge. This similar spatial tendency in the azimuthal velocities of both meddies and their sea surface expressions suggests a possible dynamic

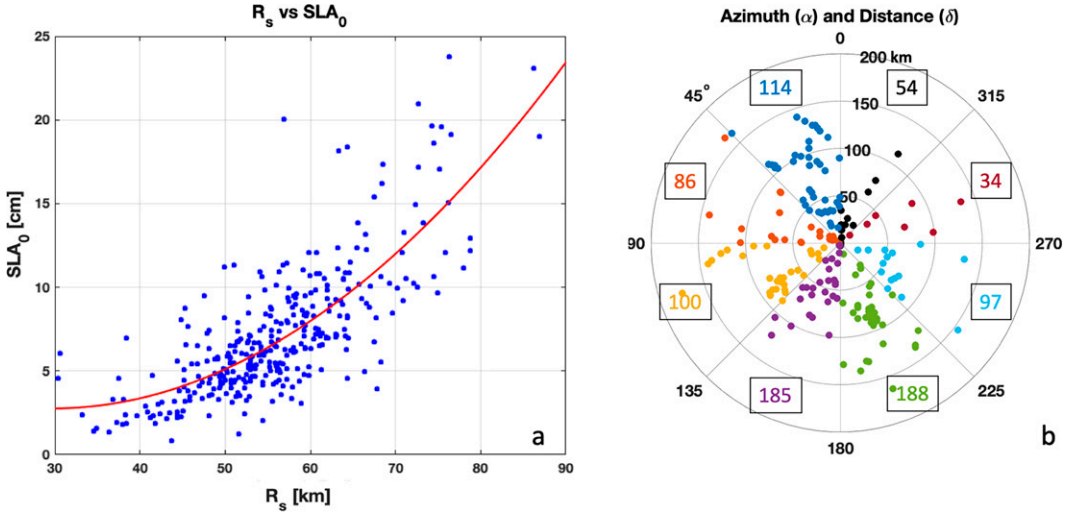

FIG. 4. (a) Radius R_s (km) plotted against the maximum sea level anomalies SLA_0 (cm) of the meddy sea surface expressions. A quadratic fit is overlaid (red curve). (b) The azimuth angle δ (°) and the separation distance α (km) between the meddy center M and the surface expression center S, subdivided by color into azimuthal octants (δ = 0°–45°; δ = 45°–90°, etc.). The respectively colored, boxed numbers in each octant show the total number of plotted values in that octant.

coupling between the properties of meddies and their sea surface signals.

The mean separation between M (derived in situ) and S (derived from AVISO altimetry) is $\overline{\delta} = 9$ km, which, considering the AVISO resolution, means that the vast majority of meddy surface signals are directly above the meddy cores. This is not immediately evident from Fig. 4b, due to repetitive overlay of the markers at small δ (many of which are equal to zero). This indicates a predominant vertical alignment of a meddy and its surface signal (or another eddy), often seen in observations and numerical models (see, e.g., Carton et al. 2013; Bashmachnikov et al. 2013; Belkin et al. 2020). A few surface signals show relatively large separation over 100 km from meddy centers, still within two radial distances between S and M. Such eddies can be considered as being coupled (Carton et al. 2016).

The azimuth angles between M and S (Fig. 4b) show a reasonably randomized distribution around the circle, with a certain tendency of S being westward or southward from M. The latter are the main directions of meddy propagation. Therefore, the surface expressions tend to stay in front of meddies moving west and south. However, meddy surface expressions can also be located at any azimuth relative to the meddy centers, consistent with numerical experiments with coupled vortices in different layers, rotating around a common center (see, e.g., Reinaud and Dritschel 2002; Bersanelli et al. 2016).

b. *Meddy sea surface expressions in measurements and in theory*

Under the quasigeostrophic approximation, the sea level elevation SLA_0 caused by the underlying core can be theoretically expressed as (Bashmachnikov and Carton 2012)

$$\mathrm{SLA}_0 = \frac{|q_m| f^2 R_m^3}{3g\, NH}, \tag{3}$$

where H is the depth of the meddy core,

$$N = \sqrt{-\frac{g}{\rho_0}\frac{\partial \rho(z)}{\partial z}}$$

is the buoyancy frequency above the meddy core, $\rho(z)$ is the water density at depth z, and ρ_0 is the reference density. The potential vorticity anomaly of the meddy core q_m, which may serve as a parameter that describes the dynamic intensity of the meddy, is defined as

$$q_m = \frac{N_m^2}{g}\,(\omega + f) - \frac{N_{\mathrm{surr}}^2}{g} f, \tag{4}$$

where $\omega = \nabla \times \mathbf{u}$ is the relative vorticity, N_m is the buoyancy frequency within the meddy core, and N_{surr} is the buoyancy frequency of the water surrounding the meddy core. In this study, we treat the meddies as isolated vortices with no interaction with surface currents—that is, with no potential vorticity anomaly above their cores.

For the majority of observations, we do not have in situ values of ω for MEDTRANS meddies. Therefore, we use a proxy term $\tilde{q}_m$ that was obtained as described in Bashmachnikov and Carton (2012), as quasigeostrophic potential vorticity, by

$$\tilde{q}_m = \frac{f}{g}(0.8N_m^2 - N_{\mathrm{surr}}^2). \tag{5}$$

The factor of 0.8 is empirically derived and assumes that the relative vorticity of a meddy is, on average, $-0.2f$. The geographical distribution of $\tilde{q}_m$ in meddy cores is plotted in Fig. 5, and the corresponding values are plotted in Fig. 6b. The $\tilde{q}_m$ values obtained are almost exclusively negative, which is typical for anticyclonic meddies. The absolute values shown in Fig. 6 are within the reasonable range expected for meddies (Tychensky and Carton 1998; Paillet et al. 2002), with an overall mean value of $\tilde{q}_m = -1.6 \times 10^{-5}\ \mathrm{s}^{-1}$.

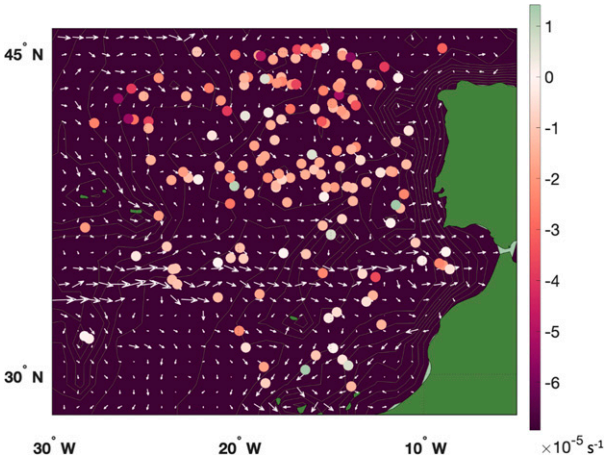

FIG. 5. Geographical distribution of quasigeostrophic potential vorticity anomalies of meddy cores ($\tilde{q}_m$; s^{-1}). Arrows mark the mean sea surface currents derived from AVISO altimetry; thin green lines show the isobaths.

We first evaluate the three exceptionally large meddy sea surface signals with SLA_0 over 20 cm (Table 1). There, we present the maximum azimuthal velocities for Rankin V_{Rn} radial velocity profiles (Carton et al. 2002):

$$V_{\mathrm{Rn}} \approx -\frac{g}{f}\frac{\mathrm{SLA}}{R_s}. \tag{6}$$

The Rayleigh V_{Ra} radial velocity profile was obtained from Eq. (6) using the expression $V_{\mathrm{Ra}} \approx V_{\mathrm{Rn}}/e^{1/2}$ (Bashmachnikov and Carton 2012). Despite the high SLA_0, the resulting velocities are in reasonable range, not exceeding 30 cm s^{-1} (Table 1). This is due to the large radii of the surface expressions, as well as to the northern position of those meddies (a larger f/N ratio). Further on we will see that the theoretical SLA_0 obtained for these northern meddies are also above the average, which suggests that these extreme SLA_0 can belong to meddy surface signals and that they are not an artifact of the method.

We thus search for any direct dependence between the parameters of the meddy sea surface signals (R_s, SLA_0) and the parameters of the meddy cores (R_m, core salinity, and core

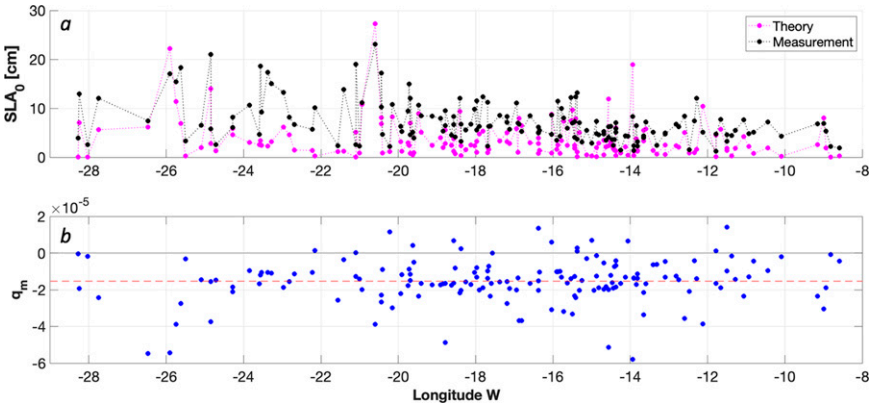

FIG. 6. (a) the measured maximum SLA_0 from AVISO satellite altimetry (black) and their theoretical estimates by Eq. (3) (magenta) for the sea surface signals of meddies marked in Fig. 2a. (b) The potential vorticity anomaly of the meddy core $|\tilde{q}_m|$ (s^{-1}) obtained from Eq. (5); the mean value is -1.6×10^{-5} s^{-1} (red dotted line).

depth), entering Eq. (3), to see whether there are some leading factors shaping the sea surface signal. In Eq. (3), R_m has the highest degree, indicating that the core radius might be the parameter upon which the meddy sea surface expressions depend most strongly. However, our results show no direct relationship between either SLA_0 or R_s and R_m (see Fig. 4, along with Fig. A1 of the appendix). The same is true for other individual parameters of the meddy cores, indicating that the basic properties of meddy sea surface expressions are not dominated by any single parameter of the meddy core.

We then compute the theoretical estimates of SLA_0 using the full Eq. (3) and compare the results with observations (Fig. 6a). With a correlation coefficient of 0.60, the results have a reasonably good agreement between the theory and observation, particularly when considering the potential error that exists in estimating different variables in Eq. (3), as well as in observations. While theory underestimates the magnitude of SLA_0 by about 50% on average, values appear to oscillate consistently, which is most clearly seen in Fig. 7. This is also seen in the regression fit described by the equation

$$SLA_{theo} = 0.56 \times SLA_0 + 0.47$$

with the determination coefficient $R^2 = 0.36$ (Fig. 7).

The relatively large scatter partly results from the possible errors in the theoretical estimates of SLA [in different parameters used in Eq. (3), especially in the potential vorticity estimated using Eq. (5)], as well as in observations (SLA is estimated from AVISO dataset, combining separated altimetry tracks). Besides the effect of these possible errors, once generated, the properties of sea surface expression parameters may become decoupled from the parameters of the underlying meddy. Typically remaining locked with the meddy below for at least several months (Bashmachnikov et al. 2009, 2015a), a meddy surface expression may then be regarded as separate eddy, the intensity and geometry of which are shaped by the immediate environment rather than by the influence of the meddy below. The latter effect can be seen when considering the geographical distributions of meddy surface expressions.

c. *Geographical distribution of meddy surface expressions*

Figure 8 shows the geographical distribution of the measured anomaly magnitude SLA_0 and radius R_s, respectively, for all output meddy surface expressions analyzed in this study. Despite the large amount of noise, one may observe a certain tendency for a westward increase in both SLA_0 and R_s (see also

TABLE 1. Parameters for the largest meddy surface (sfc) signals (1, 2, and 3 as in Fig. 2a) in measurements (meas) and theory. Presented are the surface expression magnitude SLA_0, the maximum surface azimuthal velocity of the surface expression based on Rankin V_{Rn}, and the Rayleigh V_{Ra} radial velocity profiles. For reference, the table also presents meddy core potential vorticity proxy $\tilde{q}_m$, the Coriolis parameter at the meddy core location f, and the radio of $|\tilde{q}_m|/f$ for each of the three surface signals.

	Meddy sfc signal 1		Meddy sfc signal 2		Meddy sfc signal 3	
	Meas	Theory	Meas	Theory	Meas	Theory
SLA_0 (cm)	23	27	21	14	17	22
V_{Rn} (cm s^{-1})	27	32	29	19	23	30
V_{Ra} (cm s^{-1})	16	19	18	12	14	18
$\tilde{q}_m$ (s^{-1})	-3.9×10^{-5}		-3.8×10^{-5}		-5.4×10^{-5}	
f (s^{-1})	9.8×10^{-5}		9.7×10^{-5}		9.7×10^{-5}	
$\lvert\tilde{q}_m\rvert/f$	0.40		0.39		0.56	

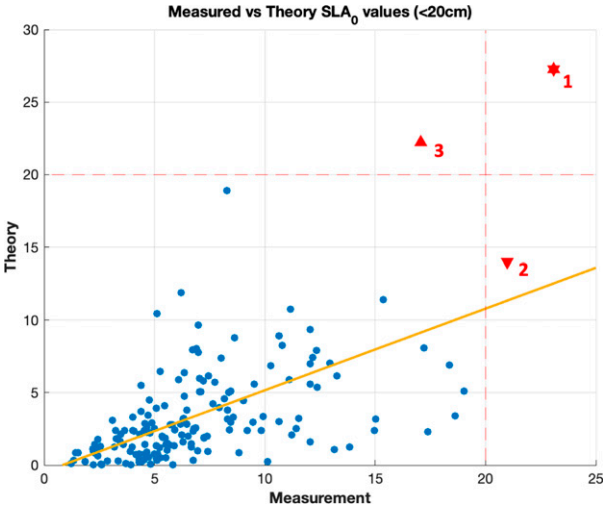

FIG. 7. Scatter diagram of the measured vs theoretically derived SLA_0 of the meddy sea surface signals (see their geographical distribution in Fig. 5). Note that the values of $SLA_0 > 20$ cm in theory (upward triangle), measurements (downward triangle), or both (six-pointed star) have been plotted in red.

Fig. 6a). Starting with values on the order of 3–6 cm near the Iberian margin, SLA_0 increases to, on average, 7–8 cm between 15° and 20°W and continues increasing westward. Similarly, the values of R_s start out at $R_s \sim 40$–50 km near the Iberian margin, and increase up to 90 km west of 20°W.

The areas of intensification of meddy surface signals in Fig. 8 match well with the locations of the main regional currents such as the Azores Current (AzC) and North Atlantic Current (NAC). This suggests a potential link between the intensities of the background current and that of the meddy surface signal.

To make the tendency for the westward increase of SLA_0 more evident, the latter is gridded onto a regular 1° × 1° grid (Fig. 9). The ratio f/N stays practically constant in the zonal direction (see Bashmachnikov and Carton 2012), whereas meddies decay and descend deeper during their westward translation, particularly west of 12°–15°W (see Bashmachnikov et al. 2015a). The latter suggests that the ratio of R_m/H decreases westward, which, on the contrary, should lead to a westward decay of the meddy surface signals.

This inconsistency may be resolved by noting a similarity between the distributions of the velocity of the mean sea surface currents and of the meddy surface expressions (Fig. 9). The surface expressions intensify in the vicinity of the mean geographical location of the Azores Current (along 34°N), as well as near the southern branch of the North Atlantic Current (at 45°N in the northwestern corner). The largest signals with $SLA_0 > 20$ cm (shown as red markers in Fig. 2a), as well as the surface signals with $SLA_0 > 15$ cm are observed in the North Atlantic Current (at approximately 43°N), and the second largest values are in the Azores Current region. The most likely explanation for this intensification of the surface expressions is that the jet currents are intensifying the meddy surface signals. This may be a result of a pulling of an anticyclonic meander over the meddy, observed in the ocean during a meddy interaction with a jet flow (see Vandermeirsch et al. 2003; Bashmachnikov et al. 2009, 2012). These interactions are out of the scope of the theory by Bashmachnikov and Carton (2012).

There is also a less distinct tendency for northward intensification, which can also be seen in the gridded SLA_0 (Fig. 9). This tendency is consistent with the theory [Eq. (3)], as the ratio f/N and the potential vorticity anomalies of the meddy cores (Fig. 5), both increase northward.

4. Discussion

The theory correctly predicts the observed northward intensification of meddy sea surface expressions, which is due to an increase of the f/N ratio. We also observe the strongest dispersion of meddy surface signals between 18° and 20°W for southern meddies, and between 15° and 17°W for the northern

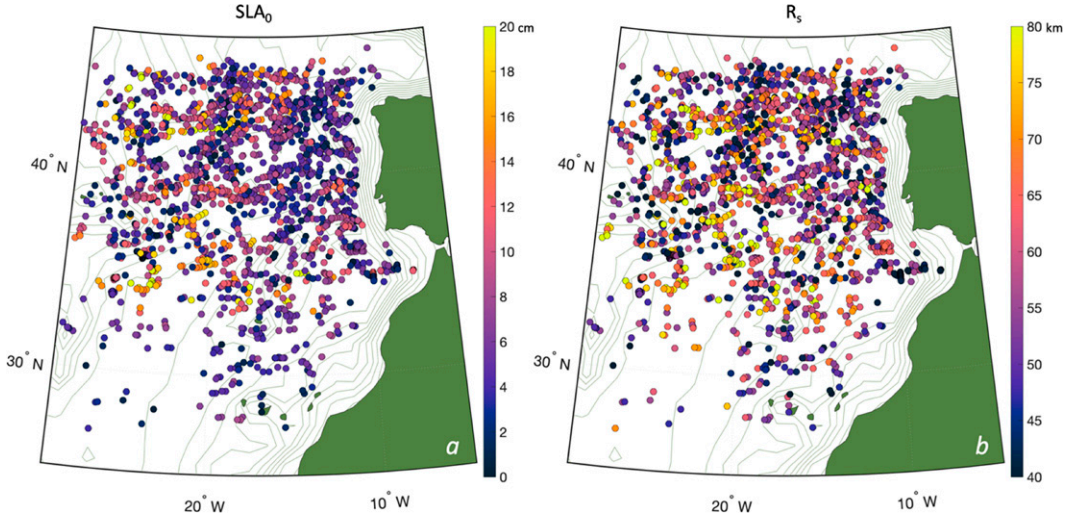

FIG. 8. Geographical distribution of the (a) maximum sea level anomaly SLA_0 and (b) radii R_s of meddy surface expressions.

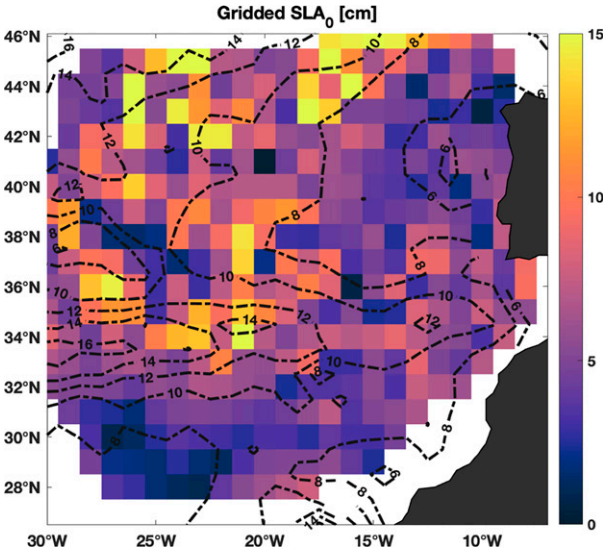

FIG. 9. Maximum SLA_0 distribution gridded onto a $1° \times 1°$ grid. Contours of the mean current magnitude is overlaid. Note the intensification of the surface expressions away from the Iberian Peninsula, with a rapid increase at around 15°–20°W.

meddies. This feature has been reported before in observations of properties of the meddy cores (see Bashmachnikov et al. 2015a) and is predicted accurately by the theory herein. In these areas, meddies reach their largest mean radii and show the highest dispersion of the radii. Along with the previously observed fact that the surface signals remain locked to meddies for extended periods of time (Bashmachnikov et al. 2009, 2013), our results suggest that there exists a certain degree of coupling between the sea surface signals and meddy core properties throughout their lifetimes (Bashmachnikov and Carton 2012).

The results of this paper suggest an important drawback of the theory. It does not consider an effect of the background current velocity on the meddy surface signals. This effect is particularly evident in the large-scale spatial distribution of the properties of meddy surface signals. Meddy cores decay in their intensity as they travel away from their formation sites at the Iberian Peninsula (Richardson et al. 2000). Meddy radii, on average, decrease after meddies leave the Canary Basin, while meddies descends to deeper levels throughout westward propagation toward the Mid-Atlantic Ridge or along the African continent (Bashmachnikov et al. 2015b). Combined together, these factors should lead to a decrease in the intensity SLA_0 and radius R_s of the meddy surface signatures with the distance from the Iberian Peninsula. However, we observe an opposing tendency of a westward intensification of meddy surface expressions and a certain increase in their radii. The areas of the most pronounced intensification correspond well to the positions of the main currents in the region: the North Atlantic and the Azores currents. This suggests that the westward growth of surface signals may be attributed to their interaction with the currents.

A background current may intensify the signal in two ways. First, a strong background flow may increase the rate of interaction of a meddy with the background ocean. Second, the dynamic instability of the main currents populates the surrounding area with surface-intensified eddies. A meddy surface signal may become distorted by interaction with such eddies, or a meddy core may become coupled with the anticyclonic sea surface structures (Vandermeirsch et al. 2003). As a result, the theoretical link between meddies and their surface expressions becomes distorted and deviates from the theoretical estimates. Jet currents or neighboring surface eddies, may intensify or reduce the intensity of the meddy surface signals, depending on a number of factors. For example, it has been repeatedly observed that, when interacting with the Azores Current, meddy surface signals first intensify, as the meddy becomes aligned with an anticyclonic meander, and then decreases to zero, as the meddy rapidly crosses the current. A reduction of the surface signal intensity has been also observed in cases were a meddy interacts with a surface cyclone, whereas interaction with an anticyclone may lead to an opposite effect (Bashmachnikov et al. 2009, 2013).

The results of this study suggest that, once generated, meddy surface expressions could be strongly shaped by the immediate environment and not by the underlying core, and that their properties become partially decoupled from the properties of the underlying meddies themselves. This could explain some of the relatively large scatter within the observed intensities of the surface signals versus their theoretical estimates (Fig. 8). The scatter also may well be due to the error involved in determining SLA_0 and R_s from altimetry observations (see, e.g., Bashmachnikov et al. 2020), as well as in the determination of various variables used in the theoretical calculation. In particular, these may originate from the estimates of $\tilde{q}_m$, for which only a proxy could be used due to a lack of observations of current velocity in the meddy core. The errors may also arise from the calculation of R_m, especially when the meddy radius is derived from a relatively small number of casts, replacing the vertically varying buoyancy frequency profiles with a mean value. Additional uncertainty arises from the method of meddy coupling with what is considered to be their surface expressions. We cannot be absolutely sure that all the detected sea surface expressions are really meddy surface signals, and some of them may be just coupled (or even uncoupled) surface eddies of other origin.

5. Conclusions

In this study we discuss whether meddy sea surface expressions are fully determined by properties of the underlying meddies that have initially generated these signals. This link follows from theoretical studies (Bashmachnikov and Carton 2012; Bashmachnikov et al. 2014; Ciani et al. 2015). We take advantage of 22 years of satellite altimetry data and the MEDTRANS database (the most complete set of historical meddy observations at this time) to correlate meddy cores with the signatures they produce at the sea surface for more than 200 meddies detected between 1993 and 2014.

In this study, a link between the intensity SLA_0 or radius R_s of the sea surface signals and some individual properties of the meddy cores, the stratification above the cores, or nondimensional numbers (the meddy aspect ratio or the f/N

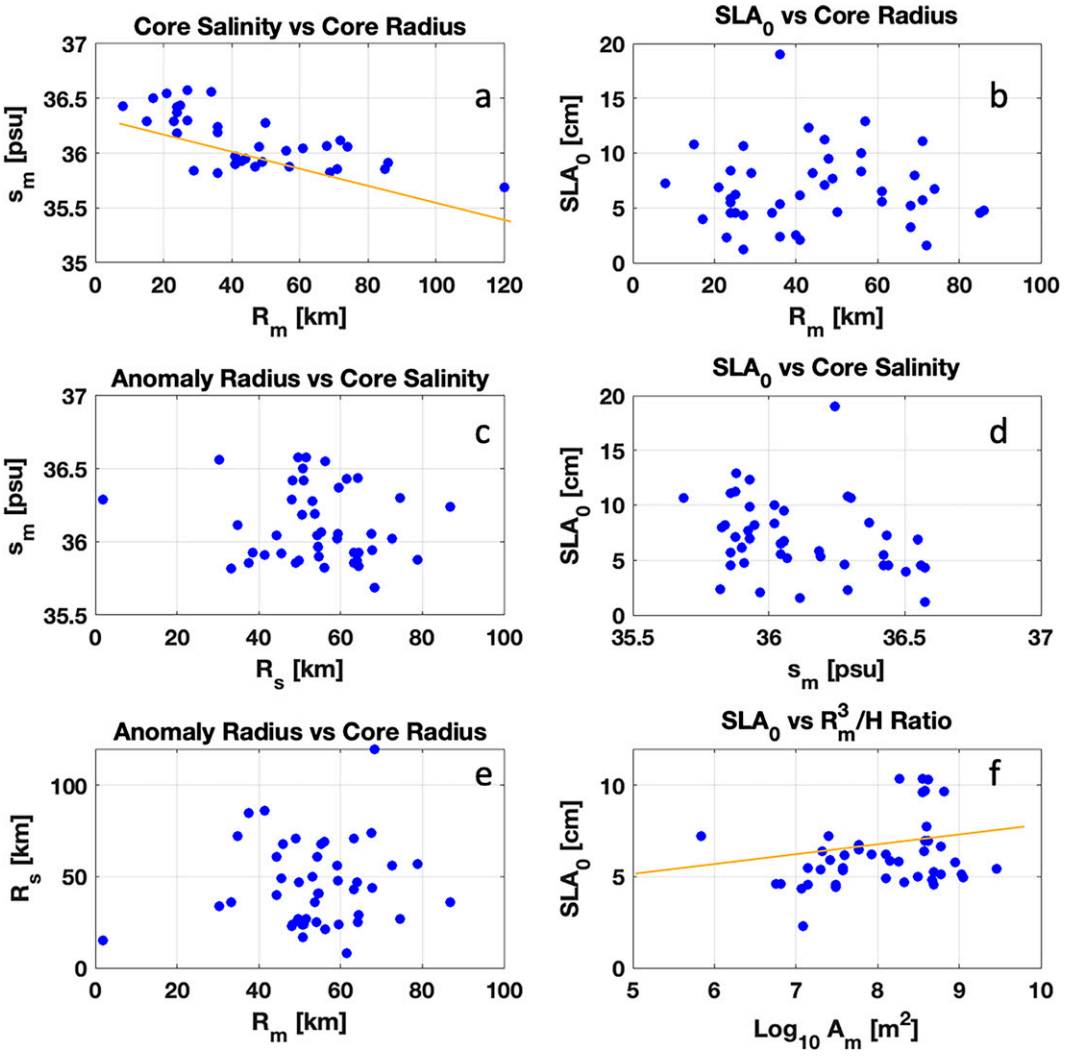

FIG. A1. Meddy core properties plotted against surface expression properties: (a) core properties R_m vs s_m, fitted linearly; (b) core and surface R_m vs SLA_0; (c) core and surface R_s vs s_m; (d) core and surface s_m vs SLA_0; (e) core and surface R_m vs R_s; and (f) core and surface SLA_0 vs $A_m = R_m^3/H$, plotted on a logarithmic scale and fitted linearly.

ratio) was initially sought. The purpose was to see whether principal properties of meddy surface signals could be defined by any individual parameter entering Eq. (3) (from Bashmachnikov and Carton 2012). The statistics obtained suggests rather a weak or no relation with any of the parameters; however, a relatively high correlation of 0.6 between the theoretical estimate of the full Eq. (3) and the observations was derived.

These results, in particular the latter result, show an overall encouraging agreement with the theory, helping to confirm the validity of both the theory and the applied method of meddy coupling with the upper-ocean anomalies. A somewhat large divergence between observations and theory does, however, exist. Some of the scatter can be attributed to errors in both the remote sensing measurements and the estimates of in situ derived variables.

Two consistent discrepancies between the observed and the theoretical datasets are derived in this study. First, the theory underestimates the sea level anomalies, on average, by a factor of 2. Second, the meddy surface signatures increase in intensity from the Iberian Peninsula to the Mid-Atlantic Ridge, while the observed evolution of the meddy cores (which, on average, become weaker, smaller and deeper, having traveled large distances along the deepening isopycnals) suggests the opposite tendency. This systematic bias should be attributed to a partial decoupling of the signal and the meddy core in a complex dynamic environment, not described by the simplified theory. In particular, we attribute the latter discrepancy to the theory not accounting for an interaction of meddies with the upper-ocean currents, as well as with eddies of different origin, both intensifying westward.

Acknowledgments. Publication of this work is supported by "Portugal Twinning for Innovation and Excellence in Marine Science and Earth Observation" (PORTWIMS) under

the European Union's Horizon 2020 research and innovation programme, Grant 810139. Author Ienna acknowledges support by Instituto Dom Luiz institute (UID/GEO/50019/2019), by the Fundação para a Ciência e Tecnologia. Author Bashmachnikov acknowledges financial support from the Russian Science Foundation (RSF), Grant 22-27-00431. Authors Dias and Ienna acknowledge financial support by FCT through MARE's strategic programme (UID/MAR/04292/2021).

Data availability statement. Data from the MEDTRANS dataset are openly available from the repository at the University of Lisbon's MARE Centre (https://www.mare-centre.pt/en/research/data-library/medtrans-data). Satellite data used in this study are available from the repository at the Archiving, Validation and Interpretation of Satellite Oceanographic data (AVISO) database via the JPL PO.DAAC website portal. Results from the meddy surface expression algorithm resulting from this study are openly available through direct contact with the corresponding author (email: fienna@fc.ul.pt) at the University of Lisbon.

APPENDIX

Additional Plots of Meddy Core Properties vs Surface Expression Properties

As an addendum to the data presented in this work, the meddy core properties measured in situ have been plotted against several surface signal properties measured by remote sensing. Figure A1 presents these plots, which can be considered in the context of the initial results shown in section 3a.

REFERENCES

Aiki, H., and T. Yamagata, 2004: A numerical study on the successive formation of Meddy-like lenses. *J. Geophys. Res.*, **109**, C06020, https://doi.org/10.1029/2003JC001952.

Arbic, B. K., R. B. Scott, D. B. Chelton, J. G. Richman, and J. F. Shriver, 2012: Effects of stencil width on surface ocean geostrophic velocity and vorticity estimation from gridded satellite altimeter data. *J. Geophys. Res.*, **117**, C03029, https://doi.org/10.1029/2011JC007367.

Arhan, M., A. C. De Verdiere, and L. Memery, 1994: The eastern boundary of the subtropical North Atlantic. *J. Phys. Oceanogr.*, **24**, 1295–1316, https://doi.org/10.1175/1520-0485(1994)024<1295:TEBOTS>2.0.CO;2.

Armi, L., and H. Stommel, 1983: Four views of a portion of the North Atlantic subtropical gyre. *J. Phys. Oceanogr.*, **13**, 828–857, https://doi.org/10.1175/1520-0485(1983)013<0828:FVOAPO>2.0.CO;2.

——, and W. Zenk, 1984: Large lenses of highly saline Mediterranean Water. *J. Phys. Oceanogr.*, **14**, 1560–1576, https://doi.org/10.1175/1520-0485(1984)014<1560:LLOHSM>2.0.CO;2.

——, D. Hebert, N. Oakey, J. F. Price, P. L. Richardson, H. T. Rossby, and B. Ruddick, 1989: Two years in the life of a Mediterranean salt lens. *J. Phys. Oceanogr.*, **19**, 354–370, https://doi.org/10.1175/1520-0485(1989)019<0354:TYITLO>2.0.CO;2.

Barbosa Aguiar, A. C., Á. Peliz, and X. Carton, 2013: A census of meddies in a long-term high-resolution simulation. *Prog. Oceanogr.*, **116**, 80–94, https://doi.org/10.1016/j.pocean.2013.06.016.

Bashmachnikov, I., and X. Carton, 2012: Surface signature of Mediterranean water eddies in the Northeastern Atlantic: Effect of the upper ocean stratification. *Ocean Sci.*, **8**, 931–943, https://doi.org/10.5194/os-8-931-2012.

——, F. Machín, A. Mendonça, and A. Martins, 2009: In situ and remote sensing signature of meddies east of the mid-Atlantic ridge. *J. Geophys. Res.*, **114**, C05018, https://doi.org/10.1029/2008JC005032.

——, D. Boutov, and J. Dias, 2013: Manifestation of two meddies in altimetry and sea-surface temperature. *Ocean Sci.*, **9**, 249–259, https://doi.org/10.5194/os-9-249-2013.

——, X. Carton, and T. V. Belonenko, 2014: Characteristics of surface signatures of Mediterranean water eddies. *J. Geophys. Res. Oceans*, **119**, 7245–7266, https://doi.org/10.1002/2014JC010244.

——, F. Neves, T. Calheiros, and X. Carton, 2015a: Properties and pathways of Mediterranean water eddies in the Atlantic. *Prog. Oceanogr.*, **137**, 149–172, https://doi.org/10.1016/j.pocean.2015.06.001.

——, ——, A. Nascimento, J. Medeiros, I. Ambar, J. Dias, and X. Carton, 2015b: Temperature-salinity distribution in the northeastern Atlantic from ship and Argo vertical casts. *Ocean Sci.*, **11**, 215–236, https://doi.org/10.5194/os-11-215-2015.

——, A. Nascimento, F. Neves, T. Menezes, and N. V. Koldunov, 2015c: Distribution of intermediate water masses in the subtropical northeast Atlantic. *Ocean Sci.*, **11**, 803–827, https://doi.org/10.5194/os-11-803-2015.

Bashmachnikov, I. L., M. A. Sokolovskiy, T. V. Belonenko, D. L. Volkov, P. E. Isachsen, and X. Carton, 2017: On the vertical structure and stability of the Lofoten vortex in the Norwegian Sea. *Deep-Sea Res. I*, **128**, 1–27, https://doi.org/10.1016/j.dsr.2017.08.001.

——, I. E. Kozlov, L. A. Petrenko, N. Glok, and C. Wekerle, 2020: Eddies in the North Greenland Sea and Fram Strait from satellite altimetry, SAR and high-resolution model data. *J. Geophys. Res. Oceans*, **125**, e2019JC015832, https://doi.org/10.1029/2019JC015832.

Belkin, I., A. Foppert, T. Rossby, S. Fontana, and C. Kincaid, 2020: A double-thermostad warm-core ring of the Gulf Stream. *J. Phys. Oceanogr.*, **50**, 489–507, https://doi.org/10.1175/JPO-D-18-0275.1.

Bersanelli, M., D. G. Dritschel, C. Lancellotti, and A. C. Poje, 2016: Models of interacting pairs of thin, quasi-geostrophic vortices: Steady-state solutions and nonlinear stability. *Geophys. Astrophys. Fluid Dyn.*, **110**, 491–517, https://doi.org/10.1080/03091929.2016.1250154.

Bower, A. S., L. Armi, and I. Ambar, 1997: Lagrangian observations of meddy formation during a Mediterranean undercurrent seeding experiment. *J. Phys. Oceanogr.*, **27**, 2545–2575, https://doi.org/10.1175/1520-0485(1997)027<2545:LOOMFD>2.0.CO;2.

Carton, X., L. Chérubin, J. Paillet, Y. Morel, A. Serpette, and B. Le Cann, 2002: Meddy coupling with a deep cyclone in the Gulf of Cadiz. *J. Mar. Syst.*, **32**, 13–42, https://doi.org/10.1016/S0924-7963(02)00028-3.

——, B. Le Cann, A. Serpette, and J. Dubert, 2013: Interactions of surface and deep anticyclonic eddies in the Bay of Biscay. *J. Mar. Syst.*, **109–110**, S45–S59, https://doi.org/10.1016/j.jmarsys.2011.09.014.

——, D. Ciani, J. Verron, J. Reinaud, and M. Sokolovskiy, 2016: Vortex merger in surface quasi-geostrophy. *Geophys.*

Astrophys. Fluid Dyn., **110**, 1–22, https://doi.org/10.1080/03091929.2015.1120865.

Chelton, D. B., M. G. Schlax, and R. M. Samelson, 2011: Global observations of nonlinear mesoscale eddies. *Prog. Oceanogr.*, **91**, 167–216, https://doi.org/10.1016/j.pocean.2011.01.002.

Ciani, D., X. Carton, I. Bashmachnikov, B. Chapron, and X. Perrot, 2015: Influence of deep vortices on the ocean surface. *Discontinuity Nonlinearity Complexity*, **4**, 281–311, https://doi.org/10.5890/DNC.2015.09.006.

——, ——, A. C. Barbosa Aguiar, A. Peliz, I. Bashmachnikov, F. Ienna, B. Chapron, and R. Santoleri, 2017: Surface signature of Mediterranean water eddies in a long-term high-resolution simulation. *Deep-Sea Res. I*, **130**, 12–29, https://doi.org/10.1016/j.dsr.2017.10.001.

CNES, 2016: SSALTO/DUACS user handbook: MSLA and (M)ADT near-real time and delayed time products. CNES Doc. CLS-DOS-NT-06-034, 29 pp., https://www.aviso.altimetry.fr/fileadmin/documents/data/tools/hdbk_duacs.pdf.

Cushman-Roisin, B., and J.-M. Beckers, 2010: *Introduction to Geophysical Fluid Dynamics: Physical and Numerical Aspects.* International Geophysics Series, Vol. 101, Academic Press, 786 pp.

——, B. Tang, and E. P. Chassignet, 1990: Westward motion of mesoscale eddies. *J. Phys. Oceanogr.*, 20, 758–768, https://doi.org/10.1175/1520-0485(1990)020<0758:WMOME>2.0.CO;2.

D'Asaro, E. A. D., 1988: Generation of submesoscale vortices: A new mechanism. *J. Geophys. Res.*, **93**, 6685–6693, https://doi.org/10.1029/JC093iC06p06685.

Demidov, A. N., B. N. Filyushkin, and N. G. Kozhelupova, 2012: Detection of Mediterranean lenses in the Atlantic ocean by profilers of the Argo project. *Oceanology*, **52**, 171–180, https://doi.org/10.1134/S0001437012020038.

Hebert, D., N. Oakey, and B. Ruddick, 1990: Evolution of a Mediterranean salt lens: Scalar properties. *J. Phys. Oceanogr.*, 20, 1468–1483, https://doi.org/10.1175/1520-0485(1990)020<1468:EOAMSL>2.0.CO;2.

Ienna, F., Y. H. Jo, and X. H. Yan, 2014: A new method for tracking meddies by satellite altimetry. *J. Atmos. Oceanic Technol.*, **31**, 1434–1445, https://doi.org/10.1175/JTECH-D-13-00080.1.

Jo, Y.-H., F. Ienna, and X.-H. Yan, 2015: An analysis of the evolution of Meddies in the North Atlantic using floats and multisensor satellite data. *J. Geophys. Res. Oceans*, **120**, 1904–1917, https://doi.org/10.1002/2014JC010495.

Käse, R. H., and W. Zenk, 1987: Reconstructed Mediterranean salt lens trajectories. *J. Phys. Oceanogr.*, 17, 158–163, https://doi.org/10.1175/1520-0485(1987)017<0158:RMSLT>2.0.CO;2.

Mauritzen, C., Y. Morel, and J. Paillet, 2001: On the influence of Mediterranean Water on the central waters of the North Atlantic Ocean. *Deep-Sea Res. I*, **48**, 347–381, https://doi.org/10.1016/S0967-0637(00)00043-1.

Mazé, J. P., M. Arhan, and H. Mercier, 1997: Volume budget of the eastern boundary layer off the Iberian Peninsula. *Deep-Sea Res. I*, **44**, 1543–1574, https://doi.org/10.1016/S0967-0637(97)00038-1.

McDowell, S. E., and H. T. Rossby, 1978: Mediterranean water: An intense mesoscale eddy off the Bahamas. *Science*, **202**, 1085–1087, https://doi.org/10.1126/science.202.4372.1085.

Morel, Y., and J. McWilliams, 1997: Evolution of isolated interior vortices in the ocean. *J. Phys. Oceanogr.*, **27**, 727–748, https://doi.org/10.1175/1520-0485(1997)027<0727:EOIIVI>2.0.CO;2.

Oliveira, P. B., N. Serra, A. F. G. Fiuza, and I. Ambar, 2000: A study of meddies using simultaneous in-situ and satellite observations. *Satellites, Oceanography and Society*, D. Halpern, Ed., Elsevier Science, 125–147.

Paillet, J., B. Le Cann, A. Serpette, Y. Morel, and X. Carton, 1999: Real-time tracking of a Galician Meddy. *Geophys. Res. Lett.*, **26**, 1877–1880, https://doi.org/10.1029/1999GL900378.

——, ——, X. Carton, Y. Morel, and A. Serpette, 2002: Dynamics and evolution of a northern meddy. *J. Phys. Oceanogr.*, **32**, 55–79, https://doi.org/10.1175/1520-0485(2002)032<0055:DAEOAN>2.0.CO;2.

Pichevin, T., and D. Nof, 1996: The eddy cannon. *Deep-Sea Res. I*, **43**, 1475–1507, https://doi.org/10.1016/S0967-0637(96)00064-7.

Piip, A. T., 1969: Large cells of Mediterranean Water in Madeira-Canaries region. *Eos, Trans. Amer. Geophys. Union*, **50**, 193.

Pingree, R. D., 1995: The droguing of meddy Pinball and seeding with ALACE floats. *J. Mar. Biol. Assoc. U. K.*, **75**, 235–252, https://doi.org/10.1017/S0025315400015332.

——, and B. Le Cann, 1993a: A shallow meddy (a smeddy) from the secondary Mediterranean salinity maximum. *J. Geophys. Res.*, **98**, 20 169–20 185, https://doi.org/10.1029/93JC02211.

——, and ——, 1993b: Structure of a meddy (Bobby 92) southeast of the Azores. *Deep-Sea Res. I*, **40**, 2077–2103, https://doi.org/10.1016/0967-0637(93)90046-6.

Reinaud, J. N., and D. G. Dritschel, 2002: The merger of vertically offset quasi-geostrophic vortices. *J. Fluid Mech.*, **469**, 287–315, https://doi.org/10.1017/S0022112002001854.

Richardson, P. L., and A. Tychensky, 1998: Meddy trajectories in the Canary Basin measured during the SEMAPHORE experiment, 1993-1995. *J. Geophys. Res.*, **103**, 25 029–25 045, https://doi.org/10.1029/97JC02579.

——, J. F. Price, D. Walsh, L. Armi, and M. Schröder, 1989: Tracking three meddies with SOFAR floats. *J. Phys. Oceanogr.*, 19, 371–383, https://doi.org/10.1175/1520-0485(1989)019<0371:TTMWSF>2.0.CO;2.

——, M. S. McCartney, and C. Maillard, 1991: A search for meddies in historical data. *Dyn. Atmos. Oceans*, **15**, 241–265, https://doi.org/10.1016/0377-0265(91)90022-8.

——, A. S. Bower, and W. Zenk, 2000: A census of Meddies tracked by floats. *Prog. Oceanogr.*, **45**, 209–250, https://doi.org/10.1016/S0079-6611(99)00053-1.

Schouten, M. W., W. P. M. De Ruijter, P. J. Van Leeuwen, and J. R. E. Lutjeharms, 2000: Translation, decay and splitting of Agulhas rings in the southeastern Atlantic Ocean. *J. Geophys. Res.*, **105**, 21 913–21 925, https://doi.org/10.1029/1999JC000046.

Serra, N., S. Sadoux, I. Ambar, and D. Renouard, 2002: Observations and laboratory modeling of meddy generation at Cape St. Vincent. *J. Phys. Oceanogr.*, **32**, 3–25, https://doi.org/10.1175/1520-0485(2002)032<0003:OALMOM>2.0.CO;2.

Shapiro, G. I., S. L. Meschanov, and M. V. Emelianov, 1995: Mediterranean lens "Irving" after its collision with seamounts. *Oceanol. Acta*, **18**, 309–318.

Sparrow, M., O. Boebel, V. Zervakis, W. Zenk, A. Cantos-Figuerola, and W. J. Gould, 2002: Two circulation regimes of the Mediterranean outflow revealed by Lagrangian measurements. *J. Phys. Oceanogr.*, **32**, 1322–1330, https://doi.org/10.1175/1520-0485(2002)032<1322:TCROTM>2.0.CO;2.

Stammer, D., H. H. Hinrichsen, and R. H. Kase, 1991: Can meddies be detected by satellite altimetry? *J. Geophys. Res.*, **96**, 7005–7014, https://doi.org/10.1029/90JC02740.

Sterlini, P., H. de Vries, and C. Katsman, 2016: Sea surface height variability in the North East Atlantic from satellite altimetry. *Climate Dyn.*, **47**, 1285–1302, https://doi.org/10.1007/s00382-015-2901-x.

Swallow, J. C., 1969: A deep eddy off Cape St Vincent. *Deep-Sea Res. Oceanogr. Abstr.*, **16** (Suppl.), 285–295.

Tychensky, A., and X. Carton, 1998: Hydrological and dynamical characterization of Meddies in the Azores region: A paradigm for baroclinic vortex dynamics. *J. Geophys. Res.*, **103**, 25 061–25 079, https://doi.org/10.1029/97JC03418.

Vallis, G., 2006: *Atmospheric and Oceanic Fluid Dynamics*. Cambridge University Press, 770 pp.

Vandermeirsch, F. O., Y. Morel, and G. Sutyrin, 2001: The net advective effect of a vertically sheared current on a coherent vortex. *J. Phys. Oceanogr.*, **31**, 2210–2225, https://doi.org/10.1175/1520-0485(2001)031<2210:TNAEOA>2.0.CO;2.

——, X. J. Carton, and Y. G. Morel, 2003: Interaction between an eddy and a zonal jet: Part II. Two-and-a-half-layer model. *Dyn. Atmos. Oceans*, **36**, 271–296, https://doi.org/10.1016/S0377-0265(02)00066-0.

Yan, X.-H., Y.-H. Jo, W. T. Liu, and M.-X. He, 2006: A new study of the Mediterranean outflow, air–sea interactions, and meddies using multisensor data. *J. Phys. Oceanogr.*, **36**, 691–710, https://doi.org/10.1175/JPO2873.1.